August 27-31, 2023
FLORENCE - ITALY
16th International Conference on Wind Engineering
ICWE 16

Influence of pivot position on the performance of a torsional flutter harvester under stationary turbulent winds

Yuhui Qin [1] and Luca Caracoglia [2]

[1]*Department of Civil and Environmental Engineering, 400 Snell Engineering Ctr., Northeastern University, 360 Huntington Avenue, Boston, MA 02115, USA, qin.yuh@northeastern.edu*
[2]*Department of Civil and Environmental Engineering, 400 Snell Engineering Ctr., Northeastern University, 360 Huntington Avenue, Boston, MA 02115, USA, lucac@coe.neu.edu*

SUMMARY:
This study investigates the linear flutter threshold instability of a torsional-flutter energy harvester in atmospheric, stationary turbulent winds. This apparatus is an example of a *flutter mill* that is a competitive alternative to similar devices of medium size, i.e., suitable as an energy supply for one or few housing units. It has a rigid blade-airfoil rotating about a pivot to generate a flapping motion. Instead of relying on the hypothesis of stochastic perturbation of mean wind speed through random stationary turbulence, the approach proposed by Scanlan (1997) for bridge flutter analysis is employed in this communication. Turbulence is introduced by suitable modification of the standard spanwise coherence equation for the aeroelastic load. Frequency domain analysis is considered to derive the incipient flutter threshold as a function of turbulence properties and pivot position. Various configurations are considered (pivot position, aspect ratio and turbulence coherence). The objective of this research is to perform a thorough sensitivity analysis as the necessary premise for the future examination of post-critical instability and operational efficiency of the harvester.

Keywords: aeroelastic harvester, flutter stability, stationary turbulence effects.

1. INTRODUCTION

In the field of wind energy, current research is directed toward offshore horizontal-axis wind turbines that optimize energy extraction at very large scales. At moderate scales, other apparatuses are often preferred because large turbines are usually less efficient, especially at moderate wind speeds. Among the various solutions, *flutter mills* have been considered. This idea has captivated the interest of the research community in the last decades; several prototypes have been analyzed (Ahmadi, 1978; Kwon et al., 2011; Matsumoto et al., 2006; Shimizu et al., 2008). For example, vibration of a flat plate with porous screens, prone to aeroelastic instability, has been considered (Pigolotti et al., 2016). Transverse vibration due to vortex shedding has also been exploited (Gkoumas et al., 2017).

Caracoglia (2018) has investigated a torsional-flutter-based apparatus for extracting wind energy (Fig. 1). The apparatus exploits the leading-edge torsional flutter instability of a blade-airfoil cross section and the magnetic induction of a coil system for energy conversion. This communication builds on the results of previous studies, which evaluated the technical feasibility and the preliminary conceptual design, to examine the effects of turbulence on flutter onset.

This paper theoretically examines the influence of three key design parameters for the apparatus. A simplified single degree of freedom (1*dof*) equation is utilized to simulate the onset of motion at flutter. The turbulence effect is considered by modelling the cross-correlation of aeroelastic loads between any two blade spanwise cross sections, which basically plays the role of aerodynamic admittance. Preliminary investigations reveal that the triggering mechanism depends on the reduced (dimensionless) frequency of the mechanical oscillator, the aspect ratio and the exponential decay parameter accounting for turbulence coherence properties.

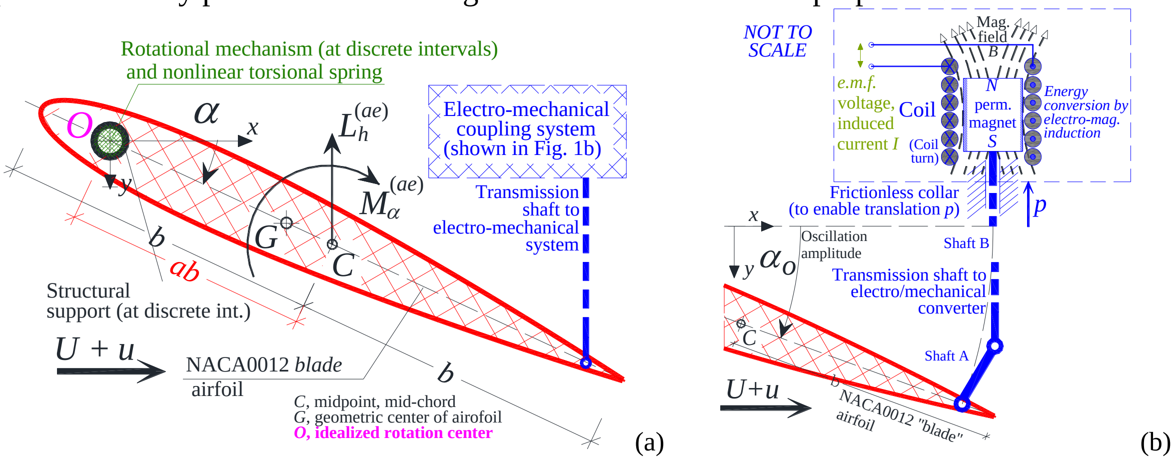

Figure 1. Schematics of the torsional flutter harvester: (a) top view, (b) energy conversion system - detail.

2. THEORETICAL BACKGROUND

The time-dependent flapping equation that models the flapping foil (rotation α) is:

$$\frac{\mathrm{d}^2\alpha}{\mathrm{d}\tau^2}+2\zeta_\alpha\frac{\mathrm{d}\alpha}{\mathrm{d}\tau}+\alpha=\frac{M_{0z}}{\omega_\alpha^2 I_{0\alpha}}-\Psi\iota \tag{1}$$

In Eq. (1) $I_{0\alpha}$ is the total polar moment of inertia of the moving components of the apparatus about pivot O (Fig. 1a); ω_α is the angular frequency of the spring-supported apparatus; $\tau=t\omega_\alpha$ is a dimensionless time variable. Structural damping is simulated through the linear term $2I_{0\alpha}\omega_\alpha\zeta_\alpha$. In Eq. (1) the excitation is provided by the total torsional aeroelastic moment M_{0z}, integrated over the spanwise length ℓ, about the pivot O. The position of the pivot is variable. Furthermore, the effect of the energy conversion apparatus (Fig. 1b) is included in Eq. (1), with ι being a dimensionless current and Ψ being a normalized electro-mechanical coupling coefficient (Caracoglia, 2018). Turbulence effects (u component in Fig. 1a) on the torque M_{0z} will be addressed below.

The mean aerodynamic moment is approximately zero. The static lift force is negligible due to blade symmetry if the static angle of attack is $\alpha\approx0$. Other loads are not considered. The unsteady moment per unit span m_{0z} is derived from classical aerodynamic theory (Bisplinghoff et al., 1955) for purely rotational motion about pole O in Fig. 1a, which can be expressed as:

$$m_{0z}=\pi\rho b^2U^2\left\{-\alpha''\left(0.125+a^2\right)+\left(2a+1\right)\alpha C(k)+\left[\left(a-0.5\right)+\left(0.5-2a^2\right)C(k)\right]\alpha'\right\} \tag{2}$$

In Eq. (2) $k=\omega b/U$ is a generic reduced frequency, $k_\alpha=\omega_\alpha b/U$ is the structural reduced frequency of the apparatus, the derivatives $\alpha'=\mathrm{d}\alpha/\mathrm{d}s$ and $\alpha''=\mathrm{d}^2\alpha/\mathrm{d}s^2$ are computed with respect to dimensionless time $s=tU/b=\tau/k_\alpha$; ρ is the air density; $C(k)=F(k)+iG(k)$ is a complex aeroelastic load function

(Theodorsen, 1935) with i being the imaginary unit. It is noted that m_{0z} is a function of k and z (spanwise coordinate) when transformed to frequency domain. At flutter onset the flapping angle is set to $\alpha(\tau)=\alpha_0 e^{i\tau/\gamma}$ (simple harmonic motion). The total aerodynamic moment thereby becomes:

$$M_{0z}=\eta_{3\mathrm{D}}\int_0^{\ell} m_{0z}(k,z)\,\mathrm{d}z=\pi\rho\eta_{3\mathrm{D}}b^2U^2\ell\gamma^{-2}k_\alpha^2\left\{\begin{matrix}-(0.125+a^2)+ik^{-1}(a-0.5)\\ +\int_0^1[\mathrm{A}_{\mathrm{E,Re}}(k,\eta)+i\mathrm{A}_{\mathrm{E,Im}}(k,\eta)]\,\mathrm{d}\eta\end{matrix}\right\}\alpha_0 e^{i\tau/\gamma} \tag{3}$$

$\mathrm{A}_{\mathrm{E,Re}}(k,\eta)=[k^{-2}(2a+1)F(k,\eta)+k^{-1}(2a^2-0.5)G(k,\eta)]$ and $\mathrm{A}_{\mathrm{E,Im}}(k,\eta)=[k^{-2}(2a+1)G(k,\eta)-k^{-1}(2a^2-0.5)F(k,\eta)]$ in Eq. (3) are real and imaginary parts of the aeroelastic load, respectively; $\eta=z/\ell$ serves as a dummy integration variable for z, accounting for the span-wise variation of the load due to turbulence effects. The "frequency ratio" is $\gamma=\omega_\alpha/\omega$, where ω is the generic angular frequency of the harmonic motion at a generic amplitude α_0. Static 3-D load effect, irrespective of turbulence, is considered through function $\eta_{3\mathrm{D}}\approx\mathrm{AR}/(\mathrm{AR}+2)$ with aspect ratio $\mathrm{AR}=\ell/b$ (Bisplinghoff et al., 1955); a finite AR yields a reduction of lift, plausible if ℓ and b are similar.

Previous work has described how to derive and solve the dynamic equation with a=-1 and for AR→∞. The goal of this research is to: (a) find the incipient flutter condition of simple harmonic motion, (b) study sensitivity of the linear aeroelastic problem. The derivation and solution are generalized to account for the variable position of the pivot axis ($a\neq-1$). If damping ratio and electric current are conservatively neglected ($\zeta_\alpha=0$, $\imath=0$) the frequency-domain dynamic problem is transformed into two equivalent algebraic equations that are solved to find the two unknown variables: the reduced frequency k^* and the angular frequency ω^* at incipient torsional flutter instability. The two equations, i.e., the real and imaginary parts of the complex-valued flutter algebraic equation, respectively are (with $\zeta_\alpha=0$, $\imath=0$, $\eta_1=z_1/\ell$, $\eta_2=z_2/\ell$):

$$\int_0^1\int_0^1 \mathrm{A}_{\mathrm{E,Re}}(k,\eta_1)\mathrm{A}_{\mathrm{E,Re}}(k,\eta_2)\,\mathrm{d}\eta_1\,\mathrm{d}\eta_2=\left[(\gamma^2-1)/(\eta_{3\mathrm{D}}\varepsilon)-\left(0.125+a^2\right)\right]^2, \tag{4}$$

$$\int_0^1\int_0^1 \mathrm{A}_{\mathrm{E,Im}}(k,\eta_1)\mathrm{A}_{\mathrm{E,Im}}(k,\eta_2)\,\mathrm{d}\eta_1\,\mathrm{d}\eta_2=\left[k\left(0.5-a\right)\right]^2. \tag{5}$$

In Eq. (4) the quantity $\varepsilon=\pi\rho b^4\ell(I_{0\alpha})^{-1}$ is a normalized inertia parameter. Using the coherence function from Scanlan (1997), the exponential decay in the aeroelastic load is expressed as:

$$\mathrm{A}_{\mathrm{E}}(k,\eta_1)\,\mathrm{A}_{\mathrm{E}}^*(k,\eta_2)=\mathrm{A}_{\mathrm{E}}(k)\mathrm{A}_{\mathrm{E}}^*(k)e^{c_0 k\mathrm{AR}/(2\pi)|\eta_1-\eta_2|} \tag{6}$$

where $\mathrm{A}_{\mathrm{E}}=\mathrm{A}_{\mathrm{E,Re}}+i\mathrm{A}_{\mathrm{E,Im}}$; $\mathrm{A}_{\mathrm{E}}^*$ is the complex conjugate of A_{E}. Thus, Eqs. (4) and (5) become:

$$\left[\mathrm{A}_{\mathrm{E,Re}}(k)\right]^2\Upsilon=\left[(\gamma^2-1)/(\eta_{3\mathrm{D}}\varepsilon)-\left(0.125+a^2\right)\right]^2,\qquad \left[\mathrm{A}_{\mathrm{E,Im}}(k)\right]^2\Upsilon=\left[k(0.5-a)\right]^2, \tag{7,8}$$

with $\Upsilon=\int_0^1\int_0^1 e^{c_0 k\mathrm{AR}/(2\pi)|\eta_1-\eta_2|}\,\mathrm{d}\eta_1\,\mathrm{d}\eta_2$ depending on k, AR and c_0; c_0 is the spanwise exponential decay parameter that varies within the range from 5 to 16 (Scanlan, 1997; Solari, 1987).

3. RESULTS: FLUTTER ONSET *VS.* TURBULENCE PROPERTIES

Equation (8) is numerically solved to find the reduced frequency at incipient flutter. It is worth noting that this equation is independent of ε, $\eta_{3\mathrm{D}}$ and γ, i.e., inertia and other system parameters have no effect on the critical reduced frequency k^*, which depends on: (*i*) position of the pivot a, (*ii*) exponential decay parameter c_0, and (*iii*) AR. Fig. 2 visualizes the surfaces of k^* and the normalized flutter speed $(k^*\gamma^*)^{-1}$ plotted in the interval of $-1.0\leq a\leq-0.7$ and $0\leq c_0\leq16$ for two aspect ratios (AR=4 and AR=10). The lower limit value c_0=0 corresponds to the turbulence-free scenario. It is shown that k^* decreases with increasing values of a and c_0. Fig. 2, in combination with the coherence function Υ, reveals that c_0 has somehow limited effect on the value of k^* due to the relatively small size of the apparatus, i.e., the reduced frequency $k^*=\omega^* b/U^*$ is small compared to other structures (e.g., bridges). In any case, the effect of c_0 is more pronounced at a larger aspect ratio. The $(k^*\gamma^*)^{-1}$ surface at AR=10 (Fig. 2c) serves as the lower bound of operational wind speed. By inspection, it is clear that for this 1*dof* flutter problem, the critical speed increases with increasing a and c_0.

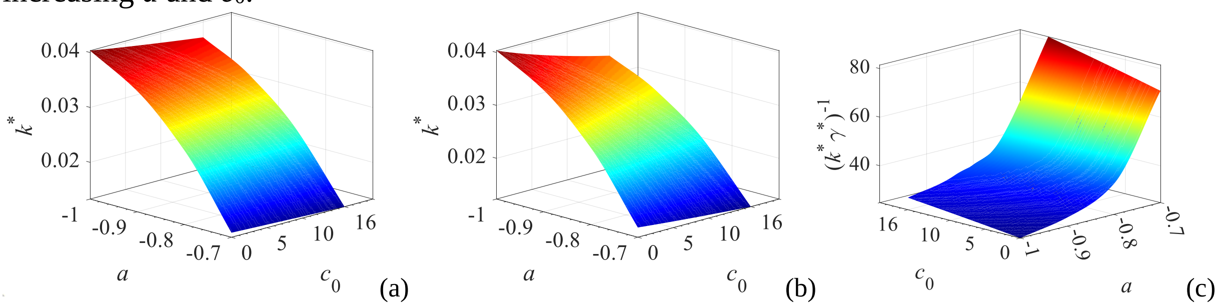

Figure 2. Effect of a and c_0 on flutter: 3-D plot of k^* with (a) AR=4, (b) AR=10; (c) flutter speed $(k^*\gamma^*)^{-1}$ at AR=10.

4. CONCLUSIONS AND OUTLOOK

The optimal pivot position to trigger flutter is found to be at a=-1.0 (Fig. 2c). The value of k^* is more sensitive to a than c_0, i.e., varying the turbulence coherence property has a relatively small effect on k^*. AR is an important design parameter that has effects on both the value of k^* and, potentially, energy conversion in the post-critical state. Frequency k^* decreases with increasing AR (Fig. 2). On the contrary, efficiency will likely increase as AR grows because the 3-D flow effect on loads is mitigated at larger AR. Therefore, AR should be meticulously examined to seek a balance between the cut-in wind velocity and the power output. While this study pertains to sensitivity to flutter onset, we intend to perform nonlinear flutter analysis in the future.

ACKNOWLEDGEMENTS

This material is based in part upon work supported by the National Science Foundation (NSF) of the United States of America, Award CMMI-2020063. Findings do not necessarily reflect the views of the NSF.

REFERENCES

Ahmadi, G., 1978. Aeroelastic wind energy converter. Energy Conversion 18, 115-120.

Bisplinghoff, R.L., Ashley, H. and Halfman, R.L., 1955. Aeroelasticity. Dover Publications Inc., Mineola, NY, USA.

Caracoglia, L., 2018. Modeling the coupled electro-mechanical response of a torsional-flutter-based wind harvester with a focus on energy efficiency examination. J. Wind Eng. Ind. Aerodyn. 174, 437-450.

Gkoumas, K., Petrini, F. and Bontempi, F., 2017. Piezoelectric vibration energy harvesting from airflow in HVAC (Heating Ventilation and Air Conditioning) systems. Procedia Eng. 199, 3444-3449.

Kwon, S.-D., Lee, H. and Lee, S., 2011. Wind energy harvesting from flutter. Proc. 13th Int. Conference on Wind Engineering (ICWE-13), Amsterdam, NL, paper No. 071 (CD-ROM).

Matsumoto, M., Okubo, K., Keisuke, M. and Ito, Y., 2006. Fundamental study on the efficiency of power generation system by use of the flutter instability. ASME Paper No. PVP2006-ICPVT-11-93773.

Pigolotti, L., Mannini, C. and Bartoli, G., 2017. Critical and post-critical behaviour of two-degree-of-freedom flutter-based generators. J. Sound Vib. 404, 116-140.

Scanlan, R.H., 1997. Amplitude and turbulence effects on bridge flutter derivatives. J. Struct. Eng. 123, 232-236.

Shimizu, E., Isogai, K. and Obayashi, S., 2008. Multiobjective design study of a flapping wind power generator. J. Fluids Eng.-ASME 130, 021104.

Solari, G., 1987. Turbulence Modeling for Gust Loading. J. Struct. Eng.-ASCE 113, 1550-1569.

Theodorsen, T., 1935. General theory of aerodynamic instability and the mechanism of flutter. Technical Report 496, National Advisory Committee for Aeronautics, Washington, DC, USA.